Journal of Applied Polymer Science

Fiber Formation by Dehydration-Induced Aggregation of Albumin

Yonnie Wu,[1] Kai Wang,[2] Gisela Buschle-Diller,[2] Mark R. Liles[3]
[1]Department of Chemistry and Biochemistry, Auburn University, Auburn, Alabama 36849-5312
[2]Department of Polymer and Fiber Engineering, Auburn University, Auburn, Alabama 36849-5327
[3]Department of Biological Sciences, Auburn University, Auburn, Alabama 36849-5312
Correspondence to: G. Buschle-Diller (E-mail: buschgi@auburn.edu)

ABSTRACT: Many proteins are capable of forming fibrils *in vitro*, suggesting that the propensity for fiber formation is a generic property of polypeptides. Pathways leading to fibril assembly, however, still remain elusive. In this research, dehydration of bovine serum albumin (BSA) solutions was found to result in spontaneous and organized formation of densely packed fibrils with the majority of proteins converted to parallel β-sheets. BSA aggregation was investigated in regard to drying conditions (airflow, temperature, and humidity) and the influence of pH, presence of anions, and protein concentration. Aggregates were prepared at large scale and cross-linked to produce water-insoluble fibers with mechanical properties comparable to those of silk. Interactions between BSA and salts suggest that removing the inner water shell surrounding globular proteins leads to protein unfolding and aggregation at the water/air interface. BSA fibers can be formed into larger assemblies such as yarns, and dyed with acid dyes, thus showing great potential for future industrial-scale applications. © 2013 Wiley Periodicals, Inc. J. Appl. Polym. Sci. 129: 3591–3600, 2013

KEYWORDS: protein β-sheet aggregation; protein dehydration; bovine serum albumin; protein–salt interaction; fibrils

Received 15 August 2012; accepted 25 October 2012; published online 1 March 2013
DOI: 10.1002/app.38771

INTRODUCTION

The dehydration of mammalian cells in culture results in the formation of structures similar in morphology to amyloidal fibrils.[1,2] Amyloidal fibrils have been known to exist in the human body for decades.[3] They are produced from diverse proteins including Aβ amyloid precursor protein, apolipoprotein A1, β2-microglobulin, transthyretin, lysozyme, huntingtin, insulin, calcitonin, alpha-synuclein, prolactin, immunoglobulin light chain, serum amyloid prion, islet amyloid polypeptide, and albumin.[4,5] The ubiquity of the cellular dehydration response in forming fibrous structures was demonstrated in many cell types,[2] yet the mechanisms responsible for cellular transformation into fibrillar morphology have not been elucidated. It has been observed that a dehydrated solution of albumin or serum results in the formation of a very similar fibril morphology.[1,2]

The study of amyloidal fibril formation in a single protein solution *in vitro* revealed that many proteins are capable of forming fibrils under specific conditions regardless of their primary sequence, indicating that the tendency to fibrillate is a generic property of the polypeptide chain.[4,6] Typically, mature fibrils consist of two to six unbranched protofilaments 2–5 nm in diameter that are associated laterally or twisted together to form larger fibrils with a diameter of 4–13 nm and a characteristic twisted, rope-like appearance.[7] Amyloids in which the β-strands are arranged perpendicular to the fibril axis contain an extended cross-β sheet central core that can be detected using X-ray diffraction (XRD).[8–10]

The pathways leading to amyloidal fibril formation, however, have yet to be fully understood.[11,12] Protein aggregates are thought to arise from interactions that normally occur intramolecularly but in this case arise in an intermolecular fashion.[13,14] The *in vitro* conditions necessary to induce fibril formation are mediated through accelerating the aggregation of unstable protein conformations, typically at low pH (2.5), high temperature (65°C), high salt content (50 m*M* NaCl), and/or with protein concentrations of less than 10 mg/mL.[7,8] These conditions are quite different from physiological conditions in blood and tissue environments (i.e., pH 7.4, 37°C, μM divalent anionic salts, more than 100 mg/mL proteins).

In addition to their medical relevance, these aggregated protein fibers have potential industrial applications. For example, products made from protein fibrils are emerging as a novel class of functional bionanomaterials[15,16]; however, scaling up their synthesis from nanoscale to macroscale to create useful macroscopic materials remains a challenge.[17] Protein fibers from non-traditional sources for textile use or incorporation in fibrous

Applied Polymer SCIENCE

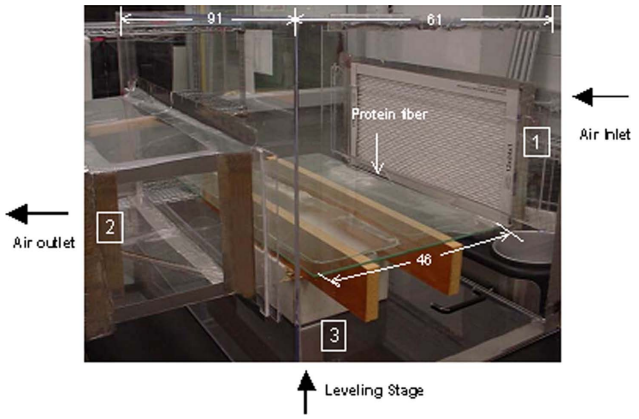

Figure 1. Dehydration box—side view, with (1) air inlet unit: control of air temperature, humidity, and angle of the air-water interface, (2) air outlet unit: control of air flow rate by moving air with a fan at three sets of speed, (3) stage leveling unit: control of the angle of the plate: slight tilt of plate allows less water in the drying front and more in the back to facilitate fiber elongation. Protein fibers are formed on the surface of a glass plate (arrow). Dimensions in cm. [Color figure can be viewed in the online issue, which is available at wileyonlinelibrary.com.]

composites have been mentioned in the literature, for instance, fibers made from milk were reported as early as 1938.[18] Yang and Reddy investigated casein fibers regenerated from alkaline solution and crosslinked with citric acid for reduced water-solubility and reasonable mechanical strength.[19] Fibers have also been made from sericin, the adhesive of silk filaments.[20–22] Although water-soluble sericin can be crosslinked with formaldehyde for reduced solubility and used by itself, in composites with other polymers, or electrospun into nanofibrous biomaterials. Fibers made from the corn protein zein were sold as textile fibers (Vicara®) in the 1960s[23] and have different potential applications.[24] Milk fibers as well as soy protein fibers have been commercialized, primarily by Asian companies.[25]

Dehydration-induced protein fibril formation is thought to result from water evaporation and induced conformational changes in protein structure. It could therefore be considered an example of dynamic self-assembly.[26] In this research, aggregation induced by dehydration of bovine serum albumin (BSA) was investigated to identify the environmental factors governing protein aggregate (i.e., fiber) formation, including the effect of ion types and concentration, pH, protein concentration, and the chemical composition of the solution. The goal is to produce novel fibers with sufficient mechanical strength and elasticity for a variety of applications. A small-scale feasibility study was performed to determine whether these BSA fibers could be made into larger assemblies, such as yarns, and dyed with acid dyes similar to traditional protein fibers, such as silk and wool, for a variety of commercial applications.

EXPERIMENTAL

Materials

BSA (Probumin®, Life Science Grade) was purchased from Millipore Corporation (Kankakee, Illinois). Dithiothreitol (DTT) was obtained from Sigma (St. Louis, Missouri) and 1-ethyl-3-[3-dimethylaminopropyl] carbodiimide (EDC) from Thermo Fisher Scientific (Waltham, Massachusetts). All other chemicals (formaldehyde, glutaraldehyde, salts, solvents, etc.) were purchased from VWR (Radnor, Pennsylvania) and were of the highest purity available.

Production of BSA Fibers

Gram quantity BSA fiber production used 200 mL solution (BSA, 10 mg/mL, 10 m*M* Na_2SO_4, 45 m*M* DTT, in Millipore water adjusted to a pH of 4.7 with HCl). The protein solution was filtered and air bubbles were removed. The protein solution was poured onto a 44 × 72 cm^2 glass surface; the desired geometry was held by surface tension. The angle of the glass plate was set by adjusting the tilting to front-high and back-low positions with no dislocation of water on the plate. The protein plate was housed in a controlled dehydration environment (Figure 1) where air temperature and humidity were held at 30°C and less than 30%, respectively. Air flow was regulated by a 3-speed WindTunnel (Power Fan, Lasko), air temperature was adjusted by an oscillate air heater (Model 5307, Lasko), and air purity was controlled by filtering the air through a microbial-free Filtrete (Ultra Allergen Air Filter-1250, 3*M*). Fibril formation was achieved by pulling air over the protein solution in a near constant laminar flow. The edge of the solution was roughened with the tip of a pipette at the beginning to enhance the nucleation that started fiber growth; dehydration and fibrillation were completed in 7 h.

Crosslinking of Protein β-Sheets by Aldehydes

The glass plate carrying the dried protein sheet was exposed to a 0.1% formaldehyde vapor in methanol overnight at room temperature in a closed environment. The fibers were then released from the glass plate by sonication in acetonitrile for 2 min, or simply scrapped off with a razor blade. Selected batches were additionally crosslinked with 0.1% aqueous glutaraldehyde solution at pH 4 at room temperature overnight. The fibers were repeatedly rinsed with methanol and air dried. Alternatively, EDC crosslinking was performed by dissolving 1 g EDC in 100 mL methanol/water (90:10) and adding 10 μL of 4*N* HCl. The BSA fibers were immersed in the solution at room temperature overnight, rinsed with methanol several times, and air dried.

Fiber Protein Composition by SDS/PAGE Gel

The protein composition of fibrils generated from BSA solution was analyzed by one-dimensional (1D) and 2D gel electrophoresis. The analysis by 1D sodium dodecyl sulfate/polyacrylamide gel electrophoresis (SDS/PAGE) used 1–10 μg proteins in 10% glycine gels, whereas 2D gel electrophoresis used 2 mg proteins in isoelectric point gel (IPG) strips (pH 3–10, PROTEAN II IPG conversion kits, Bio-Rad Laboratories, Hercules, California) for isoelectric focusing (500 V for overnight) followed by 10% polyacrylamide SDS/PAGE in PROTEAN II xi 2-D Cell (Bio-Rad; 250 V for 8 h). All gels were stained with Coomassie Blue and destained before imaging.

CR Binding

Congo Red (CR; Acros Organics, Geel, Belgium) that binds specifically to protein β-sheets was used to measure the BSA fibril concentration in an ultraviolet–visible (UV–vis) spectrophotometer (DU series 640; Beckman Coulter Fullerton, CA). All measurements were made in the wavelength range of 200–700 nm in

matched quartz cuvettes. Changes in the absorption spectra of CR before and after fibril formation in a solution of 15 μ*M* of both BSA and CR in 10 m*M* Na_2SO_4 were recorded. The average of results from three experiments was used.

Circular Dichroism

Far- and near-UV circular dichroism (CD) spectra were obtained using a JASCO-810 automatic recording spectropolarimeter (Jasco, Tokyo, Japan). Quartz cuvettes with 0.2-cm path length were used. CD spectra were obtained from aliquots taken from protein solutions at indicated conditions and recorded between 180 and 300 nm at 25°C. The molar ellipticity θ (deg cm^2 $dmol^{-1}$) was calculated from the formula: $\theta = 100\ \theta_{obs}/rlc$, where θ_{obs} is the observed ellipticity in deg, r is the amino acid residue number of the protein, l is the optical path length in cm, and c is the protein concentration in m*M*. Protein solutions were tested before fibril formation, after mixing with salts, and after being reconstituted after fibril formation. Controls included all compounds except protein for the background CD spectra. The average of eight spectra was used for all data acquisitions.

Structural Analysis with Fourier Transform Infrared Spectroscopy

Fibrils were manually crushed into powder, mixed with pulverized potassium bromide (99% spectroscopy IR grade), and formed into a solid pellet. The pellet was analyzed in absorbance mode on a Fourier transform infrared (FT-IR) (IR Prestige-21, Shimadzu) in the range of 4000–500 cm^{-1}.

XRD Diffraction

Fibers were analyzed by XRD spectra using a powder diffractometer (D8 Discover, Bruker AXS) operating at 40 kV and 40 mA using the General Area Detector. The samples were placed intact on glass slides or in form of powder and exposed to Cu K_α X-ray diffraction.

Sequencing of Cross-Linked BSA

Formaldehyde cross-linked BSA fibers, cross-linked globular BSA as well as noncross-linked native BSA as the control were tryptic digested in an enzyme to protein ratio of 1:100 (%w/w) in 10 m*M* HCl at 37°C for 24 h. The resulting soluble peptides were separated using a C18 column chromatograph ultrahigh pressure liquid chromatography (UPLC) connected to a mass analyzer (Q-TOF Premier, Waters) for both MS (peptide mapping) and MS/MS (*de novo* sequencing). Peptide ions were calibrated to mass precision at or less than 10 ppm. A 12-Dalton option was given in the sequencing algorithm that matches the modification by formaldehyde.[27]

Fiber Morphology

The microscopic methods used to investigate the morphology of the fibers were scanning electron microscopy (SEM, Zeiss EVO 50) at 20 kV on gold sputter-coated samples and light microscopy as previously described.[1,2]

Evaluation of Mechanical Properties

The mechanical properties of single fibers were tested with a Dynamics Mechanical Analyzer (RSA3, TA Instrument) measuring tensile strength. Ten individual fibers were measured from each group and their mechanical strength compared with single cotton fibers (Alabama Yarn Company) and silk fibers (experimental sample, Indonesia). Measurements were taken at room temperature (22°C) with 10-mm gauge length at 0.2 mm/min tensile speed. Calculation of strength and stress used the ribbon model (cuboids) as described in Paparcone and Buehler.[28] Young's Modulus was determined by using the stress at 1% strain. Width and thickness were measured using an optical microscope. The average of 10 measurements is represented.

Dyeing of BSA Fibers with Acid Dyes

Formaldehyde cross-linked fibers were dyed with four different Acid Dyes, including C. I. Acid Red 182, C. I. Acid Orange 7, C. I. Acid Violet 12, and C. I. Acid Blue 25. For each dyeing, 0.5 g fibers were immersed in 100 mL aqueous dye bath containing 0.02% (w/w) dye, 0.25% (w/w) Na_2SO_4 at pH 3, and a temperature of 50°C for 1 h. The fibers were rinsed in 50°C water and air-dried.

Yarn Formation

Two sets of experimental yarn were made based on 0.2 and 0.5 g BSA fibers using first an opening machine (Zellweger UsterRotorring 580) at a rotor speed of 3000 rpm to orient the fibers in parallel position. Fibers of 0.2 g were twisted at 180 turns per inch (2.54 cm) and fibers of 0.5 g were twisted at 220 turns per inch (2.54 cm). The opened fibers of 25.4 cm length were tested on a twist tester (United States Test CO. INC.) with caliper of 5.08 cm. The twist test was conducted according to the ASTM D1422 standard.

RESULTS AND DISCUSSION

Production of BSA Fibers

White and soft fiber material was prepared by BSA aggregation [Figure 2(a,b)]. Individual fibers had an average length of 35 cm and a diameter of 10–20 μm, which amounts to several orders of magnitude larger than typical amyloid fibrils.[29] The formation and quality of the BSA fibrils depended on each component in the solution mixture. Growth of fibrils occurred immediately when the liquid was drying with expanding tips pointing toward the retreating water front. This is consistent with the concept that protein aggregation must occur on the liquid side of the interface for proteins to be sufficiently mobile to stack onto the nascent growing tip. The growth appeared as an organized event [Figure 2(c)]. Molecules assembled into fibrils are hypothesized to be in a dynamic equilibrium with a pool of soluble monomers surrounding the growing tip. Fibrils extended from the nascent fine tip while simultaneously widening the maturing fibril by monomer incorporation within β-sheet aggregates. The diameter of a fibril was determined by the local dehydration rate. Slower drying allowed more time for monomers to be incorporated and resulted in fibers with larger diameters. It could be assumed that an equilibrium between globular and aggregated species developed in the evaporating solution that determined the width of each region when dried [Figure 2(d)].

Dehydration of a protein solution removes water molecules required for maintaining protein conformation, resulting in the exposure of internal hydrophobic residues and increased intermolecular interactions. A delicate balance between folded and extended protein conformations is rapidly altered when water

Applied Polymer SCIENCE

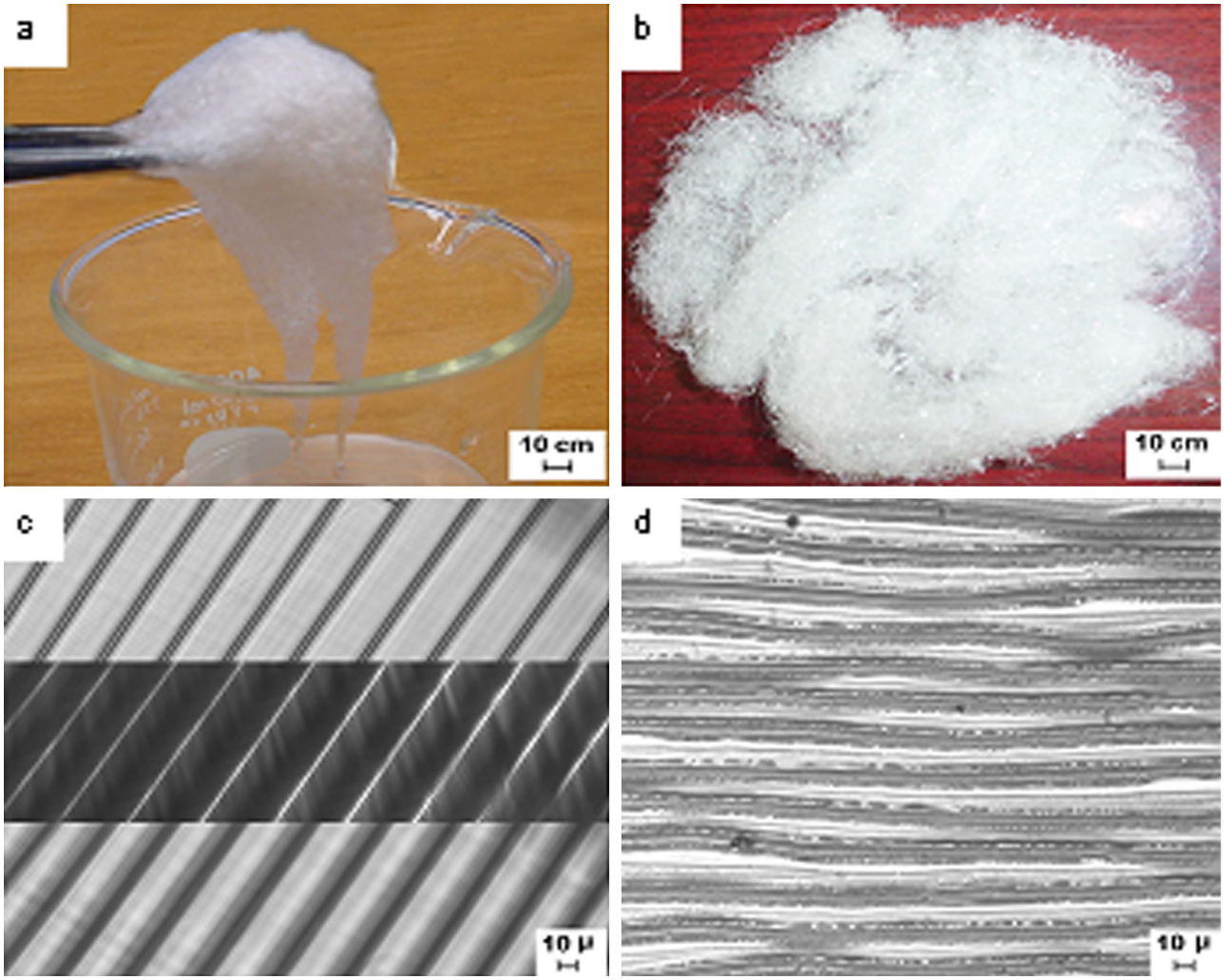

Figure 2. (a) BSA fibers harvested from glass plate after rinsing in acetonitrile solution; (b) dried BSA fibers (amount shown is 1 g); (c) optical microscopic images (magnification ×40) of longitudinal fibers superimposed on the same field with different focal points; top field: β-sheet aggregates (average width of β-sheet 9 μm), bottom field: globular form (average width 15 μm); (d) optical microscopic side view of β-sheet region with globular regions between β-sheets. [Color figure can be viewed in the online issue, which is available at wileyonlinelibrary.com.]

evaporation triggers a cascade of events in protein folding that favors an unfolded conformation and results in an ordered aggregation of proteins in cross β-sheets. Intermolecular and intramolecular interactions that maintain a protein in its native conformation are replaced by the intermolecular interactions that aggregate monomers into polymers in response to environmental factors.[14,30] In the case of the air-liquid interphase, proteins extend into β-pleated sheets through intermolecular hydrogen bonds in which neighboring polypeptide chains run in the same direction, forming a parallel β-pleated sheet. As the volume of the protein solution decreases, there is a change from a folded protein conformation to an aggregated protein conformation as a consequence of the different amount of residual water each conformation retains. It was reported that a dehydrated β-sheet structure was found in yeast amyloid-forming peptides with a reduced size.[31] The intermediate state of a partially folded amyloid protein was thought to have a larger volume than its native conformation.[32]

Regions of growth can be observed to drift where the "aggregation regions" along the length of the fibril appear more condensed than the neighboring "globular region" of albumins still in the native conformation [Figure 2(d)]. High-resolution SEM images of individual fibers revealed that fibers broke off of the large sheet in the middle of an aggregation region [Figure 3(a)] and that each fiber contained two aggregation edges along the fiber axis that have a denser texture than the globular region in the middle [Figure 3(b)]. After crosslinking with formaldehyde, these structures were no longer soluble in aqueous solution.

Straight fibrils initially formed at a slow speed, and then the rate increased considerably. The rate of fiber growth, which equaled the rate of drying, was estimated at 1.2 mm/min on average, and was 10^8 faster than that observed for amyloid formation *in vitro* when induced with low pH and high temperature.[7] The rate-limiting step in the protein conformational change seems to be dependent on solvent availability;[30] however, the rate of fibril growth was directly related to the rate of drying,

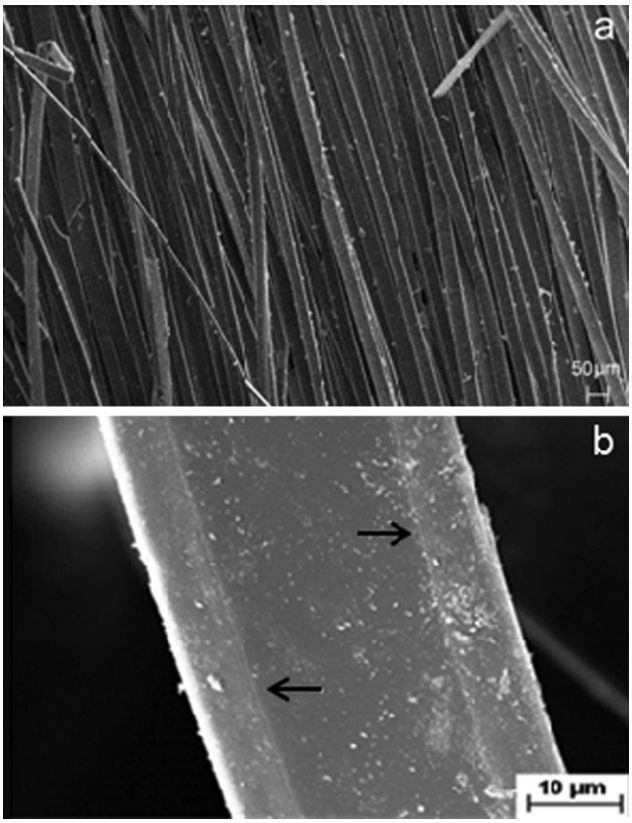

Figure 3. (a) SEM micrograph of a fibril sheet with aggregated and globular regions; (b) High-resolution SEM image of fibers with globular form in the center and β-sheet regions at both outer edges (arrows pointing at the transition areas).

which in turn is affected by air humidity, air flow (speed and volume), temperature, protein, and salt concentrations.

Without crosslinking, the fibers dissolved in water or 50% methanol but could be reformed when the water was removed with an identical structure and position which indicates that aggregation and fibril formation is a noncovalent and reversible process dependent on water availability. The cycle of fibril formation and dissolution that occurred with dehydration and rehydration was interrupted by adjusting the solution to an acidic pH (< 3), or by removing water from newly formed fibrils with acetonitrile. The type of supporting surface, either a hydrophilic glass surface or a hydrophobic polyvinyl plastic surface, did not affect fibril growth. Only the rate of fibril formation was slightly higher when a hydrophobic surface was used.

When serum had been dialyzed with a 12-KD membrane, it lost the ability to produce fibrils. However, the addition of a divalent salt (e.g., 10 m*M* Na_2SO_4) restored its capacity for fibril formation, and star-shaped fibrillar morphology similar to that previously reported for dehydrated "straw" cells[1] was observed. The impact of salt addition on fiber formation from protein solutions was therefore investigated further.

A series of 18 different inorganic and organic mono-, di- and trivalent salts were investigated in various concentrations up to 100 m*M*, such as sodium and potassium chloride, potassium iodide, sodium formate, calcium and magnesium chloride, sodium acetate, sodium and potassium phosphate, bromate, iodate and carbonate, and others. It was found that di- and trivalent anions were essential in promoting fibril formation from a pure BSA solution while monovalent anions or cations were not capable of inducing fibril genesis. Of these salts, Na_2SO_4 proved to be the most effective for fibril formation (in terms of fibril quantity) at a concentration of 10 m*M*, followed by Na_2HPO_4/NaH_2PO_4, $NaHCO_3$, and finally KIO_3 (100:15:2:1). At higher salt concentrations (50–100 m*M*), $Na_2SO_4$and Na_2HPO_4/NaH_2PO_4 became equally effective, while the other salts still resulted in less fiber formation. Ammonium sulfate, commonly used for salting out during protein purification, was not as effective as Na_2SO_4 for BSA fibril formation. Based on other studies,[33,34] Na_2SO_4 increases solvent surface tension and decreases the solubility of protein molecules (salting out), resulting in strengthened hydrophobic interactions.

The mechanism of the Hofmeister series[35] in salting out protein is not entirely clear, as multiple interactions may play a role in initiating BSA fibril growth during dehydration. Sulfate ions bind to protein at low concentrations and change the overall ionic interaction at high concentrations.[36] As water evaporates, the concentration of sulfate ions increases, the repulsive forces turn into attractive forces and the hydrophobic interactions become dominant. Although NH_4^+ is a larger ion than Na^+ in salting out protein, NH_4^+ was not as effective as Na^+ in initiating dehydration-induced fibril growth, which suggests that the mechanism is influenced by various complex factors.

Fibril formation in BSA solutions not only depends on the protein concentration but also on the pH value of the solution. In tissue, the physiological pH is effectively buffered at around 7.4, which corresponds to a low rate of fibril formation of a protein solution *in vitro*. Under slightly acidic conditions, fibrils were produced with a texture and morphology somewhat different from those at basic pH. A further increase in acidity to pH $<$ 3.5 resulted in complete inhibition of fibril formation and finally caused the protein to denature. At basic pH (>8), BSA solutions produced dramatically more, but less mechanically stable, fibrils with a peak of fibril formation observed at pH 9.0. Although a high pH value increased the solubility for most compounds, the effect could be interpreted as base-catalyzed fibril formation. Hydrogen bonds stabilize α-helix conformation to a higher extent than β-sheet. Therefore, it could be hypothesized that H-bonds could contribute to fibril formation by engaging protons originally involved in the stabilization of α-helical structures; however, these protons would preferentially stabilize globular conformation over extended cross β-sheets.

At the isoelectric point of BSA (pH 4.7), the anionic repulsion force between neighboring fibrils is lessened. At this pH, the fibril density was effectively increased, the individual fibril diameter reduced, and the conversion rate and yield were clearly enhanced. Addition of 45 m*M* DTT increased the fibril density further and shortened the distance between neighboring fibrils, thus further increasing the conversion rate and yield. DTT functions by chemically reducing BSA disulfide bonds formed from 36 cysteine residues to create a more open and linear structure,

Applied Polymer SCIENCE

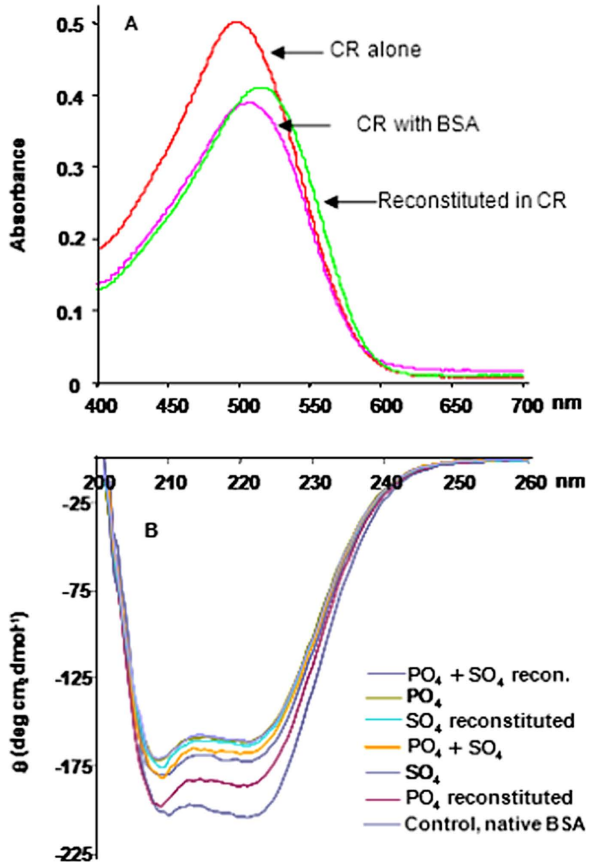

Figure 4. (a) BSA-derived fibers showing red-shifted Congo Red absorption spectra (concentration 15 μ*M*); (b) CD-spectra of BSA solutions before and after fiber formation and subsequent reformation [top to bottom: PO_4^{3-} and SO_4^{2-} (reconstituted); PO_4^{3-}; SO_4^{2-} (reconstituted); PO_4^{3-} and SO_4^{2-}; SO_4^{2-}; PO_4^{3-} (reconstituted); native BSA control]. [Color figure can be viewed in the online issue, which is available at wileyonlinelibrary.com.]

easing β-sheet formation with tight packaging into fibrils. Fibers formed at the isoelectric point showed the best mechanical properties and were studied more in detail.

Additional important factors affecting fiber formation included air flow rate and temperature during dehydration. It was found that a high constant air flow was required to produce long and dense fibrils. Slowing the air flow resulted in more amorphous aggregates with less density and more random orientation. Slow air flow also required a longer time (typically overnight) to dry a layer of protein solution at a 3-mm depth.

The optimum temperature for fibril growth was determined to be 30°C. Maintaining this temperature was important as water evaporation cooled the solution and also impacted protein aggregation in fiber formation. With all conditions and steps optimized, the final yield was at 80% (fiber weight/initial BSA weight).

Confirmation of β-Sheet Structure in BSA Fiber

Data collected from FT-IR spectroscopy of fibrils showed a peak at 1633.41 cm^{-1} indicating β-sheet structure. The peak for antiparallel β-sheet (between 1675 and 1695 cm^{-1}) was absent, suggesting that the strands within a β-sheet were parallel.[31]

CR absorption can show the β-sheet structure of a protein.[37] BSA fibrils stained with CR had an absorption shift to longer wavelengths [Figure 4(a)], confirming the presence of proteins with a β-sheet conformation when aggregated from solution. The comparison of reconstituted BSA fibrils stained with CR (15 μ*M*) with pure CR as the control indicated that fibrils before their disintegration were bound to CR causing the observed shift in the spectrum.

XRD diffraction of fibrils consisting roughly of aggregated (2/3) and globular BSA (1/3), and of fibrils in which the globular portion had been removed, showed two diffraction peaks at 3.6 and 3.2 Å corresponding to side chain amides facing the internal cavity and the repeat of amino acids in a parallel β-sheet.[9] The strand orientation for the stacked sheets was found to be perpendicular to the fiber axis. The meridional diffraction peaks appeared at 4.7 Å. The equatorial diffraction peaks at ~10 Å correspond to interstrand separation in a β-sheet and intersheet separation, respectively. These peaks were absent after dehydration-induced fibril formation which could have been the consequence of water removal.

The macroscopic β-strand aggregation resulting in fiber formation is hypothesized to be arranged perpendicularly to the fibril axis in a twisted pattern, with layers of monomers stacking onto each other, their hydrophobic residues facing outside at the air-solid interface.[38] This outward exposure of hydrophobic residues gives these fibers a smooth touch to human skin, while hydrophilic residues face inside. The hollow space in the middle of the fiber is available for holding or transporting water when rehydrated.

Fibers Made of Pure Cross β-Sheet Regions

Before formaldehyde crosslinking, fibrils could be dissolved in aqueous solution and reformed on dehydration. CD-spectra and far-UV spectrometry supported the reversible transition [Figure 4(a,b)]. In the CD-spectra [Figure 4(b)], two dips at 208 and 220 nm indicate that the loss of α-helix conformation was negligible for BSA solutions at 2 mg/mL in 10 m*M* salt solutions. Because CR-derived fluorescence intensity is a measure of fibril concentration, the observation of CR intensity before and after hydration suggests that most fibrils were in the form of globules in solution after rehydration (data not shown). The formation of fibrils through assembly of protein β-sheets was reversible up to 65°C, beyond which cross β-sheets are no longer soluble indicating an irreversible free-energy barrier in the protein folding pathway that exists once proteins are sufficiently heat denatured.

Aggregated regions could be separated from globular regions based on solubility differences in hot water. When dried BSA was briefly immersed in water of 65°C, the aggregated structure was preserved [Figure 5(a,b)] while globular albumins completely dissolved. Granules of sizes less than 1 μm could be identified in cross β-sheets. The diameter of aggregated regions varied. Pure cross β-sheet regions took the shape of either a flat ribbon or a more tubular form, indicating that variations in

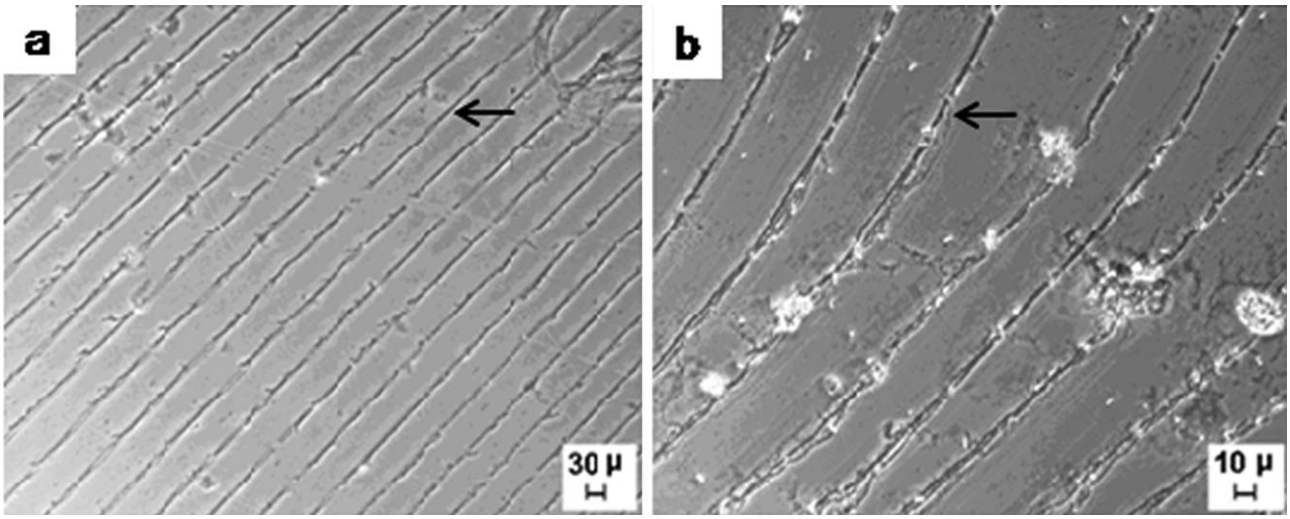

Figure 5. Light microscopic image of a BSA aggregates after removal of the globular regions by briefly washing in 65°C water (a) magnification ×10; (b) magnification ×20 (arrows pointing at the transition areas).

Table I. Mass Spectrometry Analysis of Formaldehyde-Crosslinked Amino Acids in both Aggregated and Globular BSA Molecules

m/z	Amount (ratio[a])	Peptide mapping (MS)	*De novo* sequencing (MS/MS)	Position	Modification (mass, type)
343.648^{+}	3.8	A233LK or L372AK[b]	VPK	521–523	A, 12
582.3198^{2+}	4.5	No match	TEPGALHPV**DK**	196–197	A, or B
649.142^{2+}	1.9	No match	EPHPLGPY**TMR**	207–209	A, or B
659.3618^{2+}	3.2	No match	TPVGHGG**PQNLLK**	490–492, 407–412	A, or B
727.284^{2+}	4.3	No match	TMGLVPAHNM**LNR**	480–482	A, or B
747.295^{2+}	1.9	**LGEYGFEDALLVR**[b]	**LG**$_{422}$**EYGFEDALLVR**	424–433	A, 12
784.3785^{2+}	3.1	**DAFLGSFLYEYSR**	**DAFLGSFLYEYSR**	347–359	Unmodified
1163.6398^{+}	6.6	**LVNELTEFAK**	**LVNELTEFAK**	66–75	Unmodified
1175.6296^{+}	3.1	**LVNELTEFAK**[b]	**LV**$_{67}$**NELTEFAK**	66–75	A, 12

[a]Ratio of aggregated over globular BSA of tryptic peptide ion counts that was normalized to base peak in %, [b]MS consider 12-Dalton modifications. Bold fonts are confirmed residues matching sequence.

Table II. Mechanical Properties of Individual Single BSA Fibers in Comparison of Cotton and Silk

Specimen	Yield strength (MPa)	Young's modulus (GPA)	Elongation (%)
BSA fiber at pH 6, crosslinked with formaldehyde	61 ± 16	2.71 ± 0.6	3.6 ± 1.4
BSA fiber at pH 4.7, crosslinked with formaldehyde	132 ± 30	5.31 ± 2	3.9 ± 1.6
BSA fiber at pH 4.7, crosslinked with glutaraldehyde	148 ± 4	5.72 ± 0.3	>30[a]
BSA fiber at pH 4.7, crosslinked with EDC	214 ± 97	8.26 ± 4.3	>30[a]
Cotton single fiber	77 ± 7	2.12 ± 0.4	13.8 ± 3.3
Silk single fiber	233 ± 88	4.78 ± 2	>30[a]

[a]Data beyond test limitation.

Figure 6. BSA fibers dyed with commercially available acid dyes (left to right: C.I. Acid Red 182, C.I. Acid Orange 7, C.I. Acid Blue 12, and C.I. Acid Violet 12). [Color figure can be viewed in the online issue, which is available at wileyonlinelibrary.com.]

protein aggregation existed. The yield of these fibers, however, was rather small and the fibers too short and too brittle for any practical application.

Crosslinking of BSA Fibers

Because the mechanical strength of amyloid fibrils was observed to be very low,[28,39] crosslinking could be a means to enhance their mechanical integrity and dramatically reduce their water solubility. Treatment of protein aggregates with formaldehyde resulted in crosslinking of reactive amino acids in close proximity (2.3–2.7 Å)[27] as revealed by MS and MS/MS sequencing, with quantitative differences observed between aggregated and globular proteins. Data in Table I show that peptides, spatially distant from each other in the native conformation, were closer in the aggregated cross-linked conformation.

Due to the high density of β-sheets, more aggregates were cross-linked compared to globular proteins. It can be speculated that intratype and/or intertype crosslinking (labeled as B and C in Sutherland et al., 2008)[27] have occurred nonspecifically within molecules to available residues (distance-limiting),[40] but more so to residues on surface loops (V_{62} and G_{422}, e.g.,1 and 3, as in Chen et al., 2010)[41] where amino acids are in more flexible positions.

Mechanical Properties of BSA Fibers

The mechanical properties of BSA single fibers were tested with a dynamical mechanical analyzer and were compared to those of single fibers of cotton and silk (Table II). As mentioned above, fibers were clearly stronger and much stiffer with comparable elongation if produced at the isoelectric point of BSA (pH 4.7). A second crosslinking with glutaraldehyde further increased the yield strength by ~12% at almost unchanged Young's modulus. The extensibility of the fibers, however, dramatically increased to over 30%. If EDC was used as the second crosslinking agent instead of glutaraldehyde, the fiber strength could be improved by a factor of 160%. Unfortunately, the yield strength of different fibers strongly varied as indicated by the fairly high standard deviations. Although yield strength was variable, these fibers were tougher with high elongation values. They almost reached the yield strength of silk fibers and far exceeded cotton single fiber strength, toughness, and extensibility.

Applications of BSA Fibers

The formation of fibrils from a defined protein solution on a glass surface may be a model for protein aggregation studies. Many proteins/peptides are known to form fibrils when soluble globular forms are destabilized,[31,42] thereby favoring partial unfolding and culminating in the formation of an amyloidogenic intermediate.[43,44] The influence of pH, protein concentration, water activity, and/or presence of divalent anions could affect the outcome of aggregation collectively,[45] or any one of these factors could impact aggregation dynamics. Therefore, a better understanding of protein aggregate biogenesis could contribute to the rational design of improved pharmaceuticals. Small molecular drugs targeting a protein usually bind to a specific site and as a consequence, cause a change of enzyme activity. As a protein assumes an aggregated conformation as in Alzheimer's disease, the drug must dissolve the aggregated amyloid to be effective. The BSA aggregation process could serve as

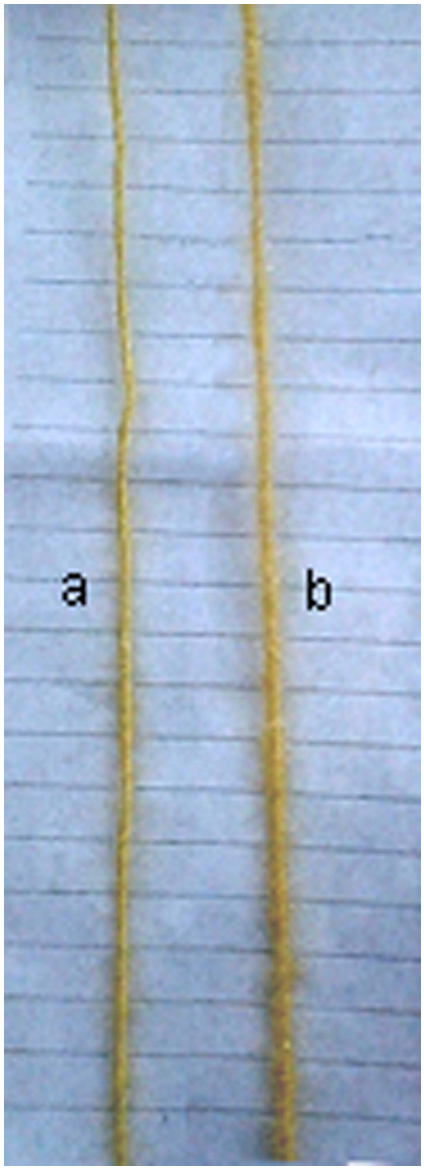

Figure 7. Assembly of BSA fibers into yarns: (a) 35-cm long BSA yarn made from 0.2 g fiber by twisting at 180 turns per 2.54 cm and (b) 35 cm long yarn made from 0.5 g fiber by twisting at 220 turns per 2.54 cm. [Color figure can be viewed in the online issue, which is available at wileyonlinelibrary.com.]

a model to support the understanding of the interaction of these small molecules with varying affinities to aggregated BSA and thus aid in the computational and experimental screening process in efficient drug design.

Varying the conditions that lead to protein aggregation has demonstrated that protein fibers can be produced in a useful size and quantity. Long fibers may be further developed for the production of novel, high-value materials with commercial utility. For instance, BSA fibers have sufficient strength and durability to be incorporated in sustainable textile composites, used as filter materials or for textile applications, to name a few potential applications.

To explore potential commercialization and to further illustrate practical versatility, it is essential that fibrous products accept colorants and form assemblies larger than single fibers. Therefore, a small-scale feasibility study was performed that included coloration experiments with BSA fibers with a number of acid dyes that are normally used for protein fibers as colorants (Figure 6). Further, simple experiments to evaluate yarn formation at two different twist levels were also carried out (Figure 7). The products of these experiments proved to be very promising and their properties will be explored in more detail in future research.

CONCLUSIONS

Fibers of good mechanical strength were made by controlled dehydration of BSA solution via an aggregation/self-assembly mechanism of stacking monomers when the forces maintaining a folded native state were removed during dehydration. Protein assembly at the air-liquid interface formed a tightly packed β-sheet fibril. Fibers formed at the isoelectric point of BSA and in the presence of Na_2SO_4 showed enhanced mechanical properties compared to fibers produced at other pH values. Formaldehyde crosslinking rendered the fibers insoluble in water. Additional crosslinking with glutaraldehyde or EDC further improved the mechanical properties of the fibers to the level of silk or better. BSA fibers were smooth and white and easily accepted conventional acid dyes. The fibers could be twisted into a yarn-like assembly and show potential as novel fibers for textile applications.

ACKNOWLEDGMENTS

The authors thank Taebum Lee (Department of Chemistry and Biochemistry, Auburn University) for the discussion of sulfate divalent anions in protein unfolding and aggregation.

REFERENCES

1. Wu, Y.; Henry, D.; Heim, K.; Tomkins, J.; Kuan, C. -Y. *BMC Cell Biol.* **2008**, *9*, 26.
2. Wu, Y.; Laughlin, R. C.; Henry, D. C.; Krueger, D. E.; Hudson, J. S.; Kuan, C. -Y.; He, J.; Reppert, J.; Tomkins, J. P. *BMC Cell Biol.* **2007**, *8*, 36.
3. Puchtler, H.; Sweat, F. A. *J. Histochem. Cytochem.* **1966**, *14*, 123.
4. Sacchettini, J. C.; Kelly, J. W. *Nat. Rev. Drug Discov.* **2002**, *1*, 267.
5. Chiti, F.; Dobson, C. M. *Annu. Rev. Biochem.* **2006**, *75*, 333.
6. Dobson, C. M. *Nature* **2003**, *426*, 884.
7. Juarez, J.; Taboada, P.; Mosquera, V. *Biophys. J.* **2009**, *96*, 2353.
8. Munishkina, L. A.; Fink, A. L.; Uversky, V. N. *J. Mol. Biol.* **2004**, *342*, 1305.
9. Perutz, M. F.; Finch, J. T.; Berriman, J.; Lesk, A. *PNAS* **2001**, *99*, 5591.
10. Perutz, M. F.; Johnson, T.; Suzuki, M.; Finch, J. T. *PNAS* **1994**, *91*, 5355.
11. Jahn, T. R.; Radford, S. E. *Arch. Biochem. Biophys.* **2008**, *469*, 100.
12. Kad, N. M.; Myers, S. L.; Smith, D. P.; Smith, D. A.; Radford, S. E.; Thomson, N. H. *J. Mol. Biol.* **2003**, *330*, 785.
13. Ashcroft, A. E. *J. Am. Soc. Mass Spectrom.* **2010**, *21*, 1087.
14. Uversky, V. N.; Segel, D. J.; Doniach, S.; Fink, A. L. *Proc. Natl. Acad. Sci. USA* **1998**, *95*, 5480.
15. Oppenheim, T. W.; Knowles, T. P. J.; Lacour, S. P.; Welland, M. E. *Acta Biomater.* **2010**, *6*, 1337.
16. Sweers, K.; Werf, K. v. d.; Bennink, M.; Subramaniam, V. *Nanoscale Res. Lett.* **2011**, *6*, 270.
17. Knowles, T. P. J.; Oppenheim, T. W.; Buell, A. K.; Chirgadze, D. Y.; Welland, M. E. *Nature Nanotechnol.* **2010**, *5*, 204.
18. R.H.O. *J. Franklin Inst.* **1938**, *225*, 620.
19. Yang, Y.; Reddy, N. *Intern. J. Biol. Macromol.* **2012**, *51*, 37.
20. Whittier, E. O.; Gould, S. P. *Ind. Eng. Chem.* **1940**, *32*, 906.
21. Zhang, X. H.; Khan, M. M. R.; Yamamoto, T.; Tsukada, M.; Morikawa, H. *Intern. J. Biol. Macromol.* **2012**, *50*, 337.
22. Zhang, Y. -Q. *Biotechn. Adv.* **2002**, *20*, 91.
23. Seymore, R. B. In The Encyclopedia of Chemistry; Clark, G. L., Reinhold Pub. Corp., New York, N.Y., Ed.; **1966**, pp 848–849.
24. Shukla, R.; Cheryan, M. *Ind. Crops. Prod.* **2001**, *13*, 171.
25. Reddy, N.; Yang, Y. *Biotechnol. Prog.* **2009**, *25*, 1796.
26. Whitesides, G. M.; Grzybowski, B. *Science* **2002**, *295*, 2418.
27. Sutherland, B. W.; Toews, J.; Kast, J. *J. Mass Spectrom.* **2008**, *43*, 699.
28. Paparcone, R.; Buehler, M. *J. Biomater.* **2011**, *32*, 3367.
29. Shammas, S. L.; Knowles, T. P. J.; Baldwin, R. L.; MacPhee, C. E.; Welland, M. E.; Dobson, C. M.; Devlin, G. L. *Biophys. J.* **2011**, *100*, 2783.
30. Myers, S. L.; Thompson, N. H.; Radford, S. E.; Ashcroft, A. E. *Rapid Commun. Mass Spectrom.* **2006**, *20*, 1628.
31. Balbirnie, M.; Grothe, R.; Eisenberg, D. S. *PNAS* **2001**, *98*, 2375.
32. White, D. A.; Buell, A. K.; Knowles, T. P. J.; Welland, M. E.; Dobson, C. M. *J. Am. Chem. Soc.* **2010**, *132*, 5171.
33. Thomas, A. S.; Elcock, A. H. *J. Am. Chem. Soc.* **2007**,*129*, 14887.

34. Zangi, R.; Hagen, M.; Berne, B. J. *J. Am. Chem. Soc.* **2007**, *129*, 4678.

35. Hofmeister, F. *Arch. Exp. Pathol. Pharmakol.* **1888**, *24*, 247.

36. Collins, K. D. *Biophys. J.* **1997**, *72*, 65.

37. Carter, D. B.; Chou, K. -C. *Neurobiol. Aging* **1998**, *19*, 37.

38. Xu, Z.; Paparcone, R.; Buehler, M. *J. Biophys. J.* **2010**, *98*, 2053.

39. Paparcone, R.; Cranford, S. W.; Buehler, M. *J. Nanoscale* **2011**, *3*, 1748.

40. Metz, B.; Kersten, G. F.; Hoogerhout, P.; Brugghe, H. F.; Timmermans, H. A.; De Jong, A.; Meiring, H.; Ten Hove, J.; Hennink, W. E.; Crommelin, D. J.; Jiskoot, W. *J. Biol. Chem.* **2004**, *279*, 6235.

41. Chen, L.; Liu, G.; Wang, Q.; Hou, W. *IEEE BMEI* **2010**, *6*, 2377.

42. Reches, M.; Porat, Y.; Gazit, E. *J. Biol. Chem.* **2002**, *277*, 35475.

43. Jarrett, J. T.; Lansbury, P. T., Jr. *Biochem.* **1992**, *31*, 12345.

44. Lomakin, A.; Teplow, D.B.; Kirschner, D.A.; Benedek, G.B. *Proc. Natl Acad. Sci. USA* **1997**, *94*, 7942.

45. Vetri, V.; D'Amico, M.; Foderà, V.; Leone, M.; Ponzoni, A.; Sberveglieri, G.; Militello, V. *Arch. Biochem. Biophys.* **2011**, *508*, 13.